

UNCLASSIFIED

AD NUMBER

AD816214

LIMITATION CHANGES

TO:

Approved for public release; distribution is unlimited.

FROM:

Distribution authorized to U.S. Gov't. agencies and their contractors; Critical Technology; JUN 1967. Other requests shall be referred to Air Force Technical Applications Center, Washington, DC. This document contains export-controlled technical data.

AUTHORITY

usaf ltr, 25 jan 1972

THIS PAGE IS UNCLASSIFIED

AD816214

MULTIPLE COHERENCE OF SHORT PERIOD NOISE AT LASA

26 June 1967

Prepared For

AIR FORCE TECHNICAL APPLICATIONS CENTER
Washington, D. C.

By

E. F. Chiburis
W. C. Dean

TELEDYNE, INC.

Under

Project VELA UNIFORM

Sponsored By

ADVANCED RESEARCH PROJECTS AGENCY
Nuclear Test Detection Office
ARPA Order No. 624

**BEST
AVAILABLE COPY**

MULTIPLE COHERENCE OF
SHORT PERIOD NOISE AT LASA

SEISMIC DATA LABORATORY REPORT NO. 190

AFTAC Project No.:	VELA T/6702
Project Title:	Seismic Data Laboratory
ARPA Order No.:	624
ARPA Program Code No.:	5810
Name of Contractor:	TELEDYNE, INC.
Contract No.:	F 33657-67-C-1313
Date of Contract:	2 March 1967
Amount of Contract:	\$ 1,736,617
Contract Expiration Date:	1 March 1968
Project Manager:	William C. Dean (703) 836-7644

P.O. Box 334, Alexandria, Virginia

AVAILABILITY

This document is subject to special export controls and each transmittal to foreign governments or foreign national may be made only with prior approval of Chief, AFTAC.

This research was supported by the Advanced Research Projects Agency, Nuclear Test Detection Office, under Project VELA-UNIFORM and accomplished under the technical direction of the Air Force Technical Applications Center under Contract F 33657-67-C-1313.

Neither the Advanced Research Projects Agency nor the Air Force Technical Applications Center will be responsible for information contained herein which may have been supplied by other organizations or contractors, and this document is subject to later revision as may be necessary.

TABLE OF CONTENTS

	Page No.
ABSTRACT	
1. INTRODUCTION	1
2. DESCRIPTION OF DATA	5
3. RESULTS	6
Multiple Coherences	6
Power Spectra	8
Stationarity Tests	10
4. CONCLUSIONS	12
FIGURES	
APPENDIX 1	1-1
Multiple Coherence Functions	
APPENDIX 2	2-1
Theoretical Development of The Stationarity Relations	
A. Noise Reduction Within The Fitting Interval	2-1
B. Noise Reduction Outside The Fitting Interval	2-3
REFERENCES	

ABSTRACT

Multiple coherence gives a quantitative measure versus frequency of how well a linear combination of n input channels can match the $(n + 1)$ st channel in a seismic array. If the inputs can match the output exactly, then the multiple coherence is unity and only n channels are necessary to describe the noise field. This report shows multiple coherence versus frequency with 2 to 9 input channels for short period noise fields at LASA.

Intersubarray noise from the center seismometers in the 500-foot holes at LASA shows low multiple coherence for all frequencies from 0.1 to 2.5 cps even with the closest subarrays represented. The intersubarray multiple coherence indicates that the expected noise reduction from a prediction error filter is about 1 db over the fitting interval and about 0 db outside the fitting interval.

Intrasubarray noise has a high multiple coherence for frequencies of 1 cps and lower when some input channels are within $\frac{1}{2}$ km of the output channel. When the inputs are at least 2 km away, the multiple coherence is less than 0.8 for all but micro-seismic frequencies.

1. INTRODUCTION

Most basic data processing techniques for signal enhancement or identification depend upon the structure of the noise within the seismic array. If some of the coherent noise is due to site characteristics such as consistently coherent noises from particular directions, then techniques using multiple coherence will help to isolate these consistent linear relations. Many optimum filters for estimating the signal take account of these linear relations implicitly by weighting with the inverse of the spectral noise matrix. However, one cannot tell whether the coherent noise involved is due to noise generating events which cannot be predicted or controlled. Thus, the filters must be recalculated over a period of noise recording immediately prior to the arrival of each single signal. Part of the coherent noise generated within the array may be due to various causal factors for a particular array. If so, we can learn something about these factors by examining the linear relations between the various array elements. A potential benefit here is that a consistent linear model relating the different sub-elements would eliminate the need for computing a different set of filter coefficients for each event.

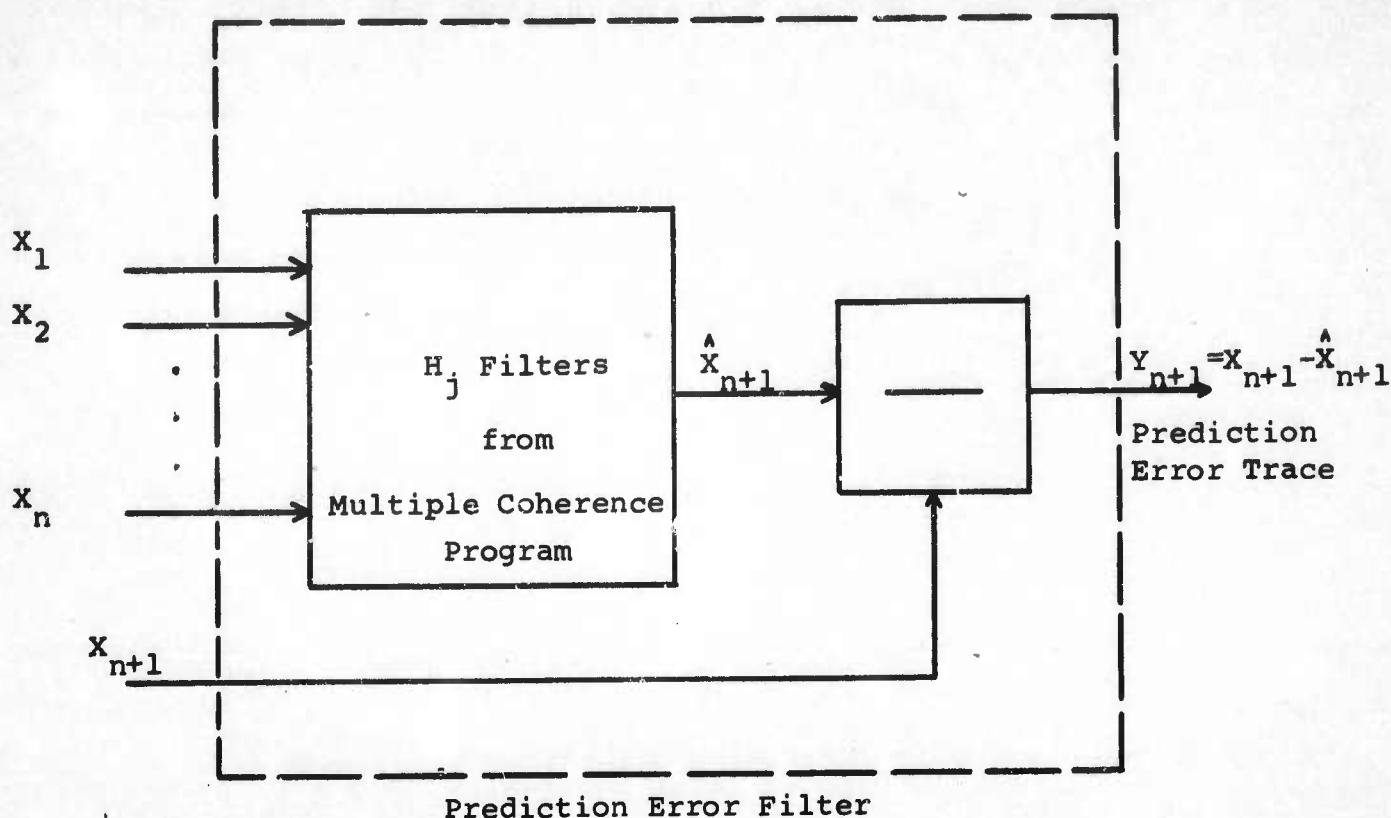
The multiple coherence function can indicate how many seismometer outputs in an array are necessary to properly determine the seismic noise field. If there are n independent seismic noise components, then the multiple coherence function would be unity when $(n + 1)$ st seismometers are placed in an array to measure seismic noise records. If part of the background is

composed of incoherent noise, then the multiple coherence function would indicate the percentage of coherent noise present and the number of seismometers necessary to define this coherent noise. The filter relations determined by the multiple coherence computations can then be used in array summation to bring the noise into destructive interference.*

This analysis does not guarantee that such optimum processing is possible. For example, if the noise and signal propagation characteristics across the array are identical, no velocity filtering scheme can be expected to separate the two even though the multiple coherence might be unity.

The multiple coherence function is the frequency domain equivalent of the prediction error filter in time. If n input seismic traces predict the $(n + 1)$ st trace in an array completely, then the multiple coherence will be unity and a prediction error filter could be used to exactly predict this $(n + 1)$ st output. In fact, linear filter relations derived by the multiple coherence program produce an estimate of the $(n + 1)$ st trace which, when subtracted from the actual $(n + 1)$ st trace, gives a prediction error trace. Thus the combination of the filter derived in the multiple coherence program and the subtraction operation produces a prediction error filter as shown in the following diagram.

*For the mathematical description of the multiple coherence computation, see Appendix I.



The first objective of this study is to use the multiple coherence function to estimate the degree of predictability of the short period noise field at LASA. The result in turn should tell us how much the noise power should be reduced by optimum filtering (e.g., maximum likelihood or Wiener filters) if the filters were theoretically ideal.

The second objective is to determine from multiple coherences the number of independent components comprising a given noise field and the percentage of incoherent noise which cannot be cancelled by any kind of multichannel filtering.

The third objective is to determine the stationarity properties of the noise field. We accomplish this by applying the multiple coherence program to three different time samples from the same array. Then the multiple coherency filters derived

from the first time sample are applied to the other two time samples. If the filters derived in the first time sample have done a good job of predicting the noise field in all three samples, then the data are said to be stationary. On the other hand, if the filters from the first time sample do a progressively poorer job of predicting the noise in the other samples relative to the filters associated with those samples, then the noise is non-stationary to some degree. This deterioration in predictability of the multiple coherence filter can quantitatively measure the non-stationarity of the data**.

**For a theoretical discussion of the stationarity computation, see Appendix II.

2. DESCRIPTION OF DATA

We computed the multiple coherences of short-period LASA data for both within the subarray (intrasubarray) and between subarrays (intersubarray). The noise within a subarray was tested for subarray A0. The output seismometer was the center element, A010. The multiple coherence was computed as a function of frequency and the number of inputs. The first inputs added were from the outermost ring. The number of input channels increases from 2 to 9. The multiple coherence is plotted versus frequency with the number of input channels as a parameter. Since adding one additional channel to the set of inputs may not increase but can never decrease the amount of input information about the noise field, the multiple coherence must be a monotonically increasing function with increasing number of inputs.

In computing the multiple coherences between subarrays, the center elements from each subarray were used. Again the output trace was from the center of the array, subarray A0. The ordering of the input channels was done in two ways. In the first, we added the outer most channels first and the near ones last; in the second, we reversed this procedure.

The noises examined were three successive signal-free samples, eight minutes long, recorded on 25 March 1966. In addition, stationarity tests were made on these samples. Also tested were one signal-free sample and one sample including LONGSHOT from 29 October 1965.

3. RESULTS

Multiple Coherences

Figure 1 shows intersubarray multiple coherences versus frequency for two time samples chosen 8 minutes apart for 25 March 1966. A diagram of the array elements chosen is shown in the center of the figure. The ordering of the inputs is from outermost to closest and is shown in the figure. The multiple coherences are computed every .1 cps over a range from .2 to 2.6 cps. The number of points in each sample is 4799. The number of lags computed in the correlation function is 200. The data sampling rate is 10 points per second.

The intersubarray multiple coherences are seen to be low over the entire frequency range for even as many as 9 inputs. The number of lags used in the correlation is sufficient to detect any propagating noise component with a velocity greater than 1.25 km per second. This velocity limitation may affect the correlation between A0 and the D-ring. However, most of the inputs are closer than 15 km so that the lack of sufficient lags to detect significant correlations is not a cause for the low multiple coherences observed.

Figure 2 shows the multiple coherences versus frequency for both inter- and intrasubarray noise from a sample on 29 October 1965. The subarray and array diagrams are shown in the center of the figure, and the ordering of the inputs is again from the outermost to the closest.

The intersubarray noise still shows low coherences although the values for all 10 inputs are somewhat above those plotted in Figure 1. The intrasubarray coherences are quite large out to 1 cps when 7 or more inputs are used. However, the 7th, 8th and 9th

inputs are only $\frac{1}{2}$ km away from the output trace so high coherences are to be expected. When the closest inputs are 2 km away, however, the multiple coherences are significantly less than .8 for almost all frequencies. Here again, the number of lags is sufficient to detect any propagating noise components that could exist.

Figure 3 shows the multiple coherences for the same inter-subarray data given in Figure 2. In this case, the ordering of the inputs adds the closest seismometers first. The final multiple coherence trace with all 10 inputs must still be, and is, the same as the final trace on Figure 2. We find, however, that even using the closest seismometers first, we do not approach this final multiple coherence any faster. This result shows that the intersubarray noise at LASA is essentially incoherent.

As a demonstration that the multiple coherence program will detect significant correlations when they do exist, we have shown the intrasubarray multiple coherence when the noise field contains a seismic signal. The upper diagram in Figure 4 shows the multiple coherence within a subarray when the LONGSHOT event was recorded. Here the multiple coherence is above .8 for most frequencies with 5-6 inputs, and is essentially unity with 9 inputs. The lower diagram in Figure 4 shows similar multiple coherences when the data contains a smaller seismic signal. Here the multiple coherence is reduced because the signal is weaker compared to the incoherent background than in the case of LONGSHOT. Even so, the multiple coherence for this weaker signal plus noise is significantly above the multiple coherence for noise alone within a subarray.

Figure 5 shows intersubarray multiple coherences for the LONGSHOT and Andreanof events similar to the intrasubarray coherences of Figure 4. The multiple coherences on Figure 5 show striking differences from those of Figure 4. The intrasubarray coherences are highest at the low frequencies and somewhat lower over the middle frequencies. On Figure 5 the lowest frequencies show low coherences and quite high coherences around the middle frequencies. This result can be explained by considering the signal-to-noise ratios. At the lowest frequencies we have noise only. Over intrasubarray distances the microseismic noise is coherent whereas over intersubarray distances it is not. Over the middle frequencies where the signal spectra are strongest, the noise is weakest for the intersubarray case since the inputs are all from 500 foot holes. Consequently, signal-to-noise ratios from the intersubarray case especially for the Andreanof event, is much higher and the multiple coherences consequently, much higher than for the intrasubarray events.

Power Spectra

Spectra for the multiple coherence examples on Figures 1-4 are presented on Figures 6-10 and Figures 12 and 13. Figure 6 shows the output spectra at A0 and the range of input spectra for 9 intersubarray inputs from the first noise sample on March 25, 1966.

Figure 7 shows the spectra from the same 500-foot holes shown in Figure 6 but computed with 100 instead of 200 lags. The variation in lags shows essentially no difference in the power spectra.

In Figure 8 the power spectra shown for the third time sample are similar to those shown for the first in Figure 6.

Figure 9 shows the output and input power spectra for the intrasubarray noise sample immediately preceding the LONGSHOT event. Figure 10 shows the similar spectra for the intersubarray noise prior to LONGSHOT. The two output traces in Figure 9 and 10 are identical.

A marked difference between the input spectra for the higher frequencies shows up between Figures 9 and 10. The intrasubarray spectra (Figure 9) are from 200-foot holes and show appreciably higher energy near 2 cps than do the intersubarray spectra from 500-foot holes shown in Figure 10. The spectral difference between the 20C and 500 foot seismograms implies that the intrasubarray multiple coherence might be improved, particularly at the higher frequencies, if we would use an output trace from a 200-foot hole. Figure 11 shows the intrasubarray multiple coherence when the output is from a 200-foot hole $\frac{1}{2}$ km from the center seismometer. Except for this difference in output traces this case corresponds to that shown in the upper half of Figure 2. In comparing the two we find virtually no difference whatever between the multiple coherences for any frequency in these two cases. Furthermore, the multiple coherences versus frequency for these two cases agree regardless of the number of input channels used.

Figure 12 shows the output and input spectra for the interval including the LONGSHOT event.

Figure 13 shows the input and output spectra for the interval including the Andreanof earthquake.

Stationarity Tests

The multiple coherence program derives a set of n filters for the n input seismograms which together provide the best linear estimate for the $(n + 1)$ st seismic trace. The difference between the observed $(n + 1)$ st trace and the best estimate is the error trace. If the multiple coherence is unity, the prediction is perfect and the error trace will be zero. If we form the ratio of the error spectra over the observed spectra, we can get a measure of the reduction in noise power possible from the theoretical optimum filters. Thus the db improvement as a function of frequency can be expressed as

$$db = 10 \log (\text{error/observed}).$$

The prediction error filters will do the best job in eliminating the noise background when they are applied to the noise sample from which they are derived. However, if the noise is stationary, the same filter could be expected to do nearly as well when applied to later time samples from the same array. Figure 14 shows the expected noise reduction in db when the prediction error filters that were derived from the first time sample are applied to the first time sample. In addition these same filters are applied to the second and third time samples. The three 8-minute time samples are adjacent to each other. Figure 14 shows that the reduction of the noise background from a prediction error filter can be expected to be between .5 and 2 db. The same filter applied to the second and third time sample gives 0 db and thus shows no reduction of the noise background whatever. This small amount of noise reduction of intersubarray data is to be expected when the multiple coherence is less than 30%.

Figure 15 shows similar results when filters derived from the second time sample are applied to all three. This expected noise reduction and lack of stationarity is further evidence that the noise is essentially incoherent.

4. CONCLUSIONS

1. Intersubarray noise at LASA shows a low multiple coherence over all frequencies, even with 9 input channels.

2. Even the closest subarrays at LASA show little coherency.

3. Intrasegment noise at LASA shows a high multiple coherence for frequencies of 1 cps and lower when 7 or more inputs are used. However, the 7th, 8th, and 9th inputs are only $\frac{1}{2}$ km away from the output trace. When the closest inputs are 2 km away from the output, the multiple coherences are significantly less than .8 for all but microseismic frequencies.

4. The digital programs will show high coherence and multiple coherence when present e.g., LONGSHOT event has high multiple coherence over subarrays. An Andreanof earthquake, a weaker event than LONGSHOT, shows multiple coherences between those of LONGSHOT and noise-only cases.

5. Low multiple coherence is not due to insufficient lags. The programs have sufficient resolution to handle noise propagation with velocity, 1 km/sec and less.

6. Power spectra from the seismometers at 500 feet agree with those at 200 feet only out to 1.2 cps. Beyond this frequency the power spectra density of the deeper seismometers continue to fall, while the power spectra densities from the shallow seismometers rise.

7. The multiple coherence using shallow seismometers as inputs trying to match the deeper seismometer as output falls rapidly beyond 1.2 cps.

8. The intrasegment multiple coherence using shallow seismometers as both inputs and output is approximately the same as for intrasegment multiple coherences which uses the trace from the 500-foot hole as output. This result is obtained in spite

of a striking difference in the power spectra of the shallow and deep seismograms.

9. The intersubarray multiple coherence indicates that the expected noise reduction from a prediction error filter is about 1 db over the fitting interval and about 0 db outside the fitting interval.

FIGURES

1. Intersubarray multiple coherences versus frequency for two short period samples recorded at LASA on 25 March 1966.
2. Multiple coherences versus frequency for both inter and intrasubarray noise recorded at LASA on 29 October 1965.
3. Multiple coherences versus frequency for the intersubarray data shown on Figure 2 but with the closest seismometers added first.
4. Intrasubarray multiple coherences versus frequency for the LONGSHOT event and an Andreanof earthquake event.
5. Intersubarray multiple coherences versus frequency for the LONGSHOT events.
6. Output and range of input spectra for intersubarray samples used on Figure 1.
7. Output and range of input spectra for intersubarray samples used on Figure 1 but computed with 100 instead of 200 lags.
8. Output and range of input spectra for the third time sample similar to those presented on Figure 6.
9. Output and range of input spectra for the intrasubarray noise immediately preceding the LONGSHOT event.
10. Output and range of input spectra for the intersubarray noise immediately preceding the LONGSHOT event.
11. Intrasubarray multiple coherence versus frequency when the output is from a seismometer in a 200 foot hole instead of the 500 foot hole at the subarray center.
12. Output and range of input spectra for the interval including the LONGSHOT event.
13. Output and range of input spectra for the interval including the Andreanof earthquake event.
14. Expected noise reduction in db when a prediction error filter is applied to the fitting interval (Time 1) and the two adjacent intervals.
15. Expected noise reduction in db when a prediction error filter is applied to the fitting interval (Time 2) and the two adjacent intervals.

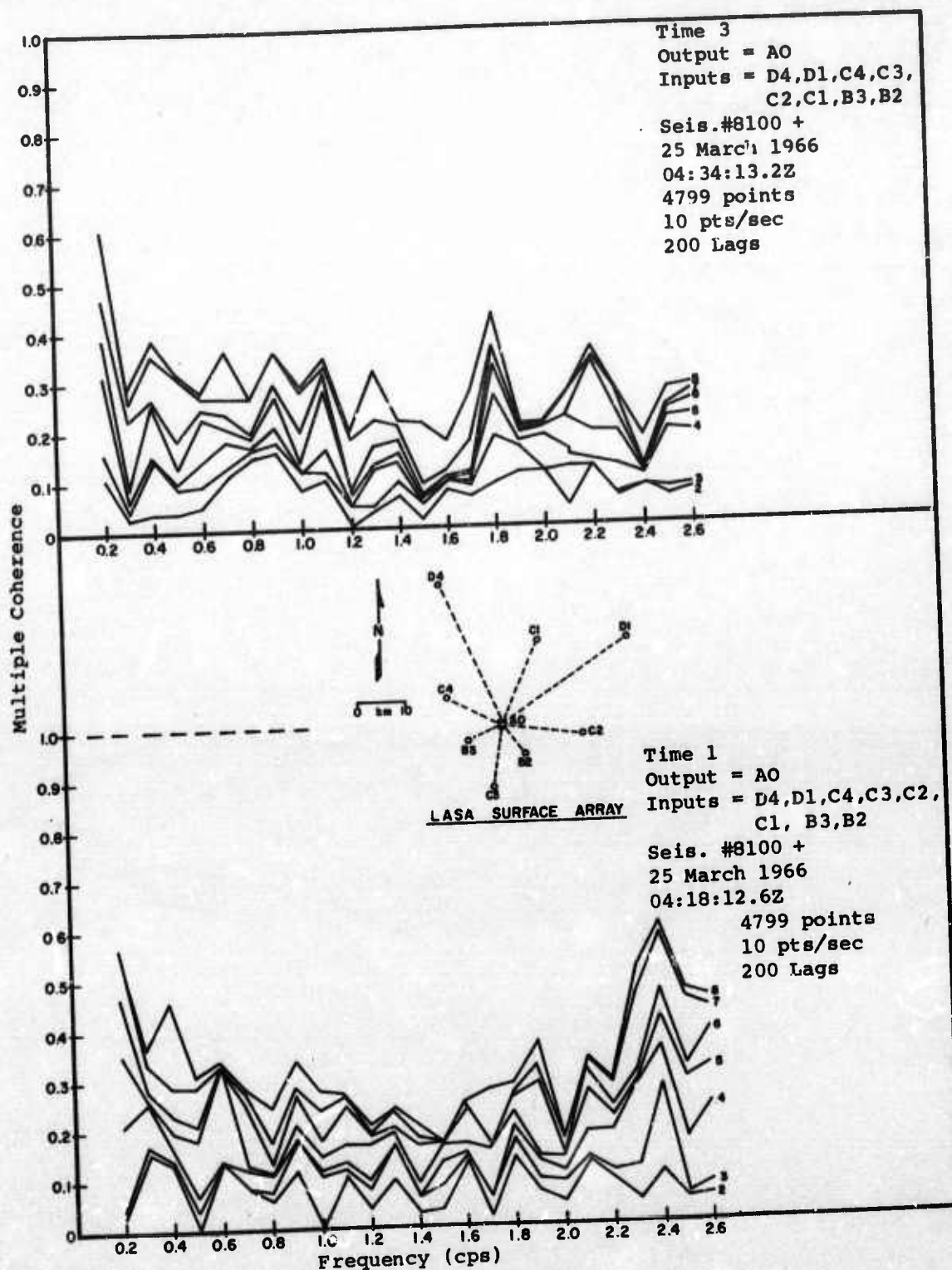


Figure 1. Intersubarray multiple coherences versus frequency for two short period samples recorded at LASA on 25 March 1966.

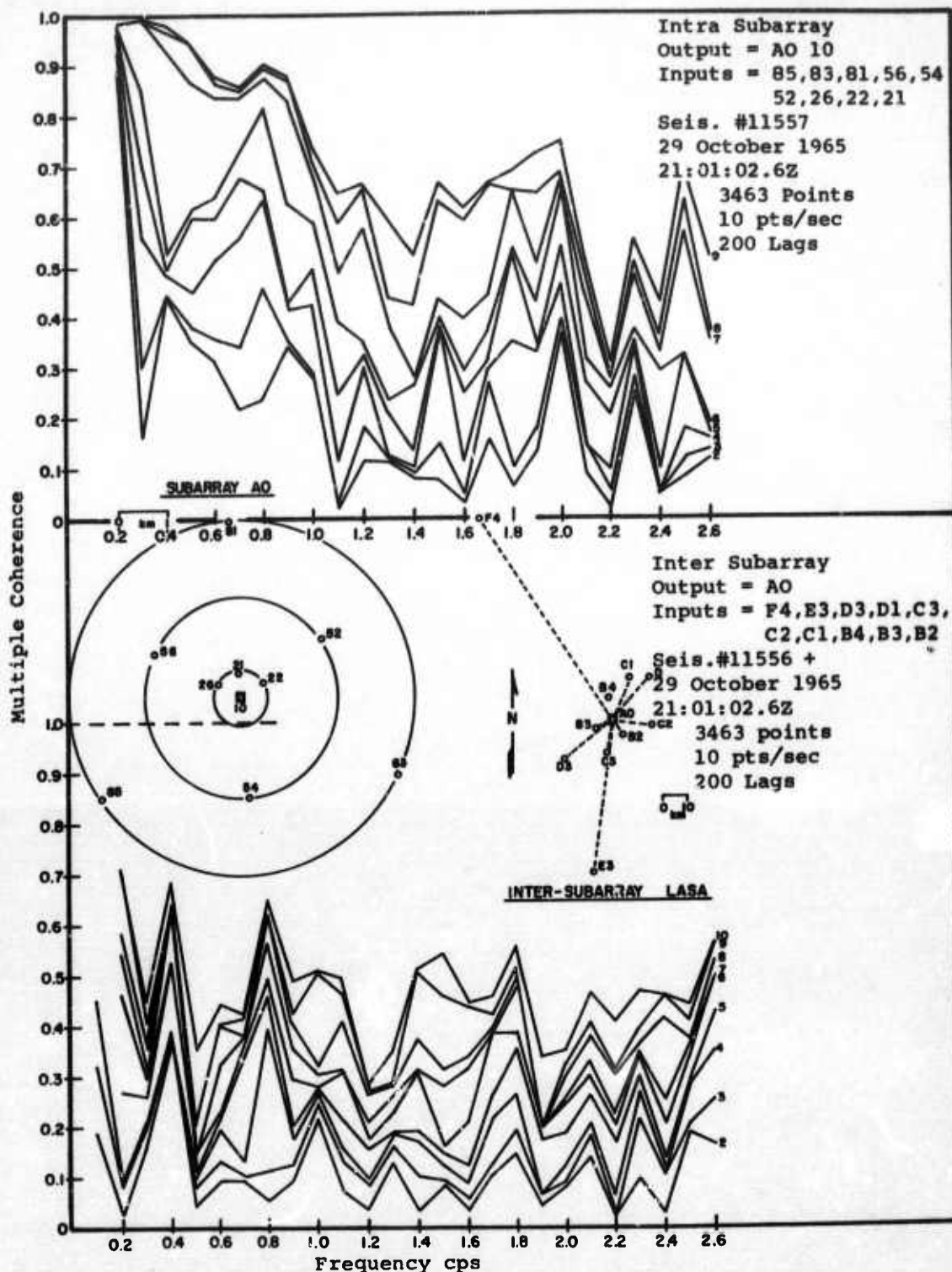


Figure 2. Multiple coherences versus frequency for both inter and intrasubarray noise recorded at LASA on 29 October 1965.

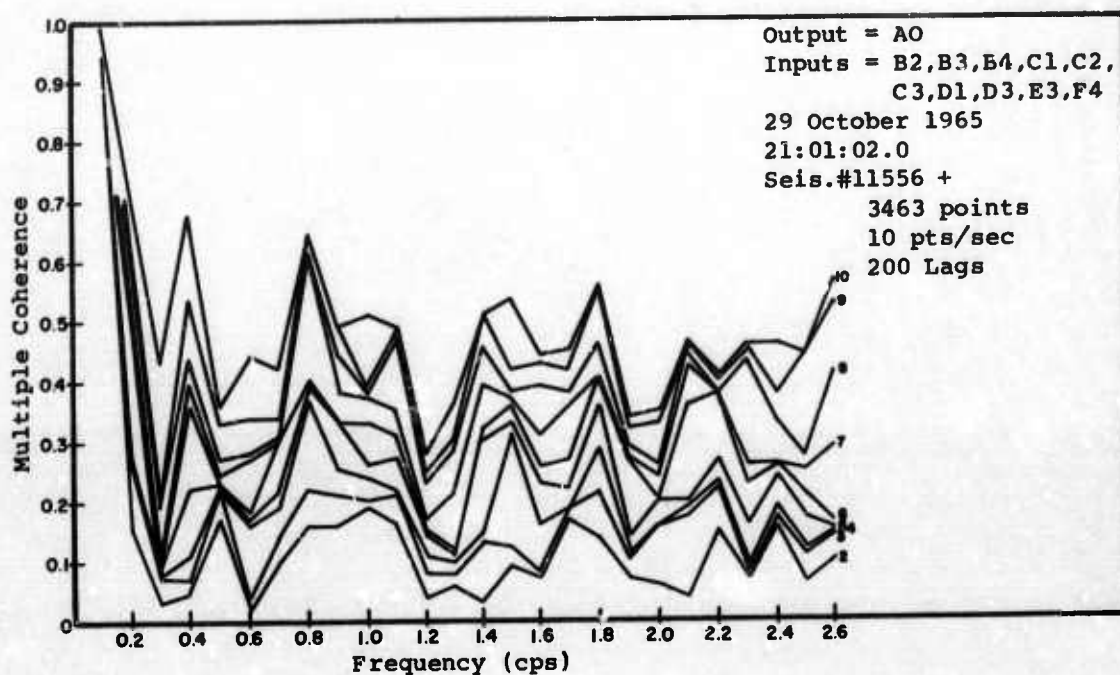


Figure 3. Multiple coherences versus frequency for the inter-subarray data shown on Figure 2 but with the closest seismometers added first.

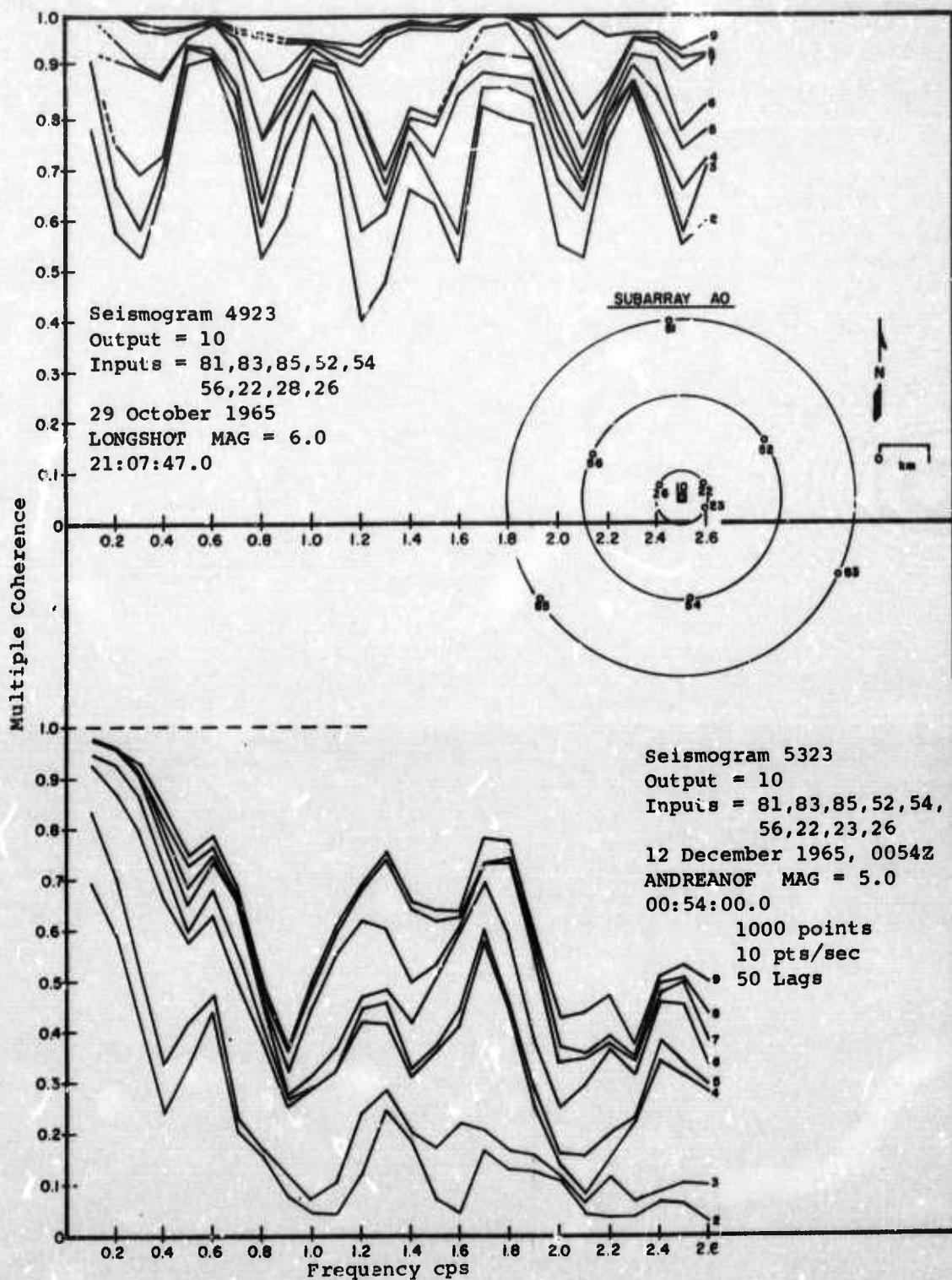


Figure 4. Intrasubarray multiple coherences versus frequency for the LONGSHOT event and an Andreanof earthquake event.

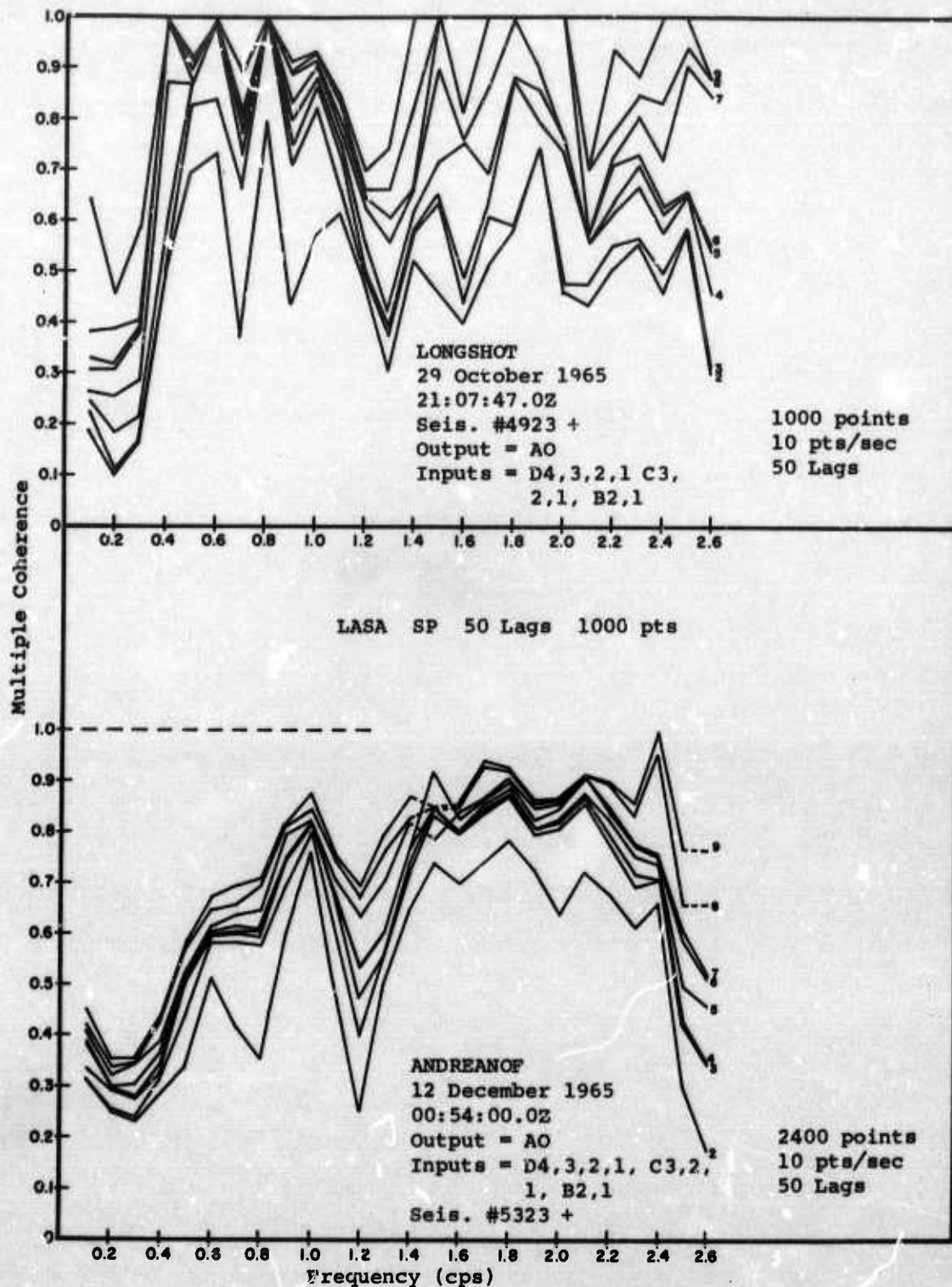


Figure 5. Intersubarray multiple coherences versus frequency for the LONGSHOT events.

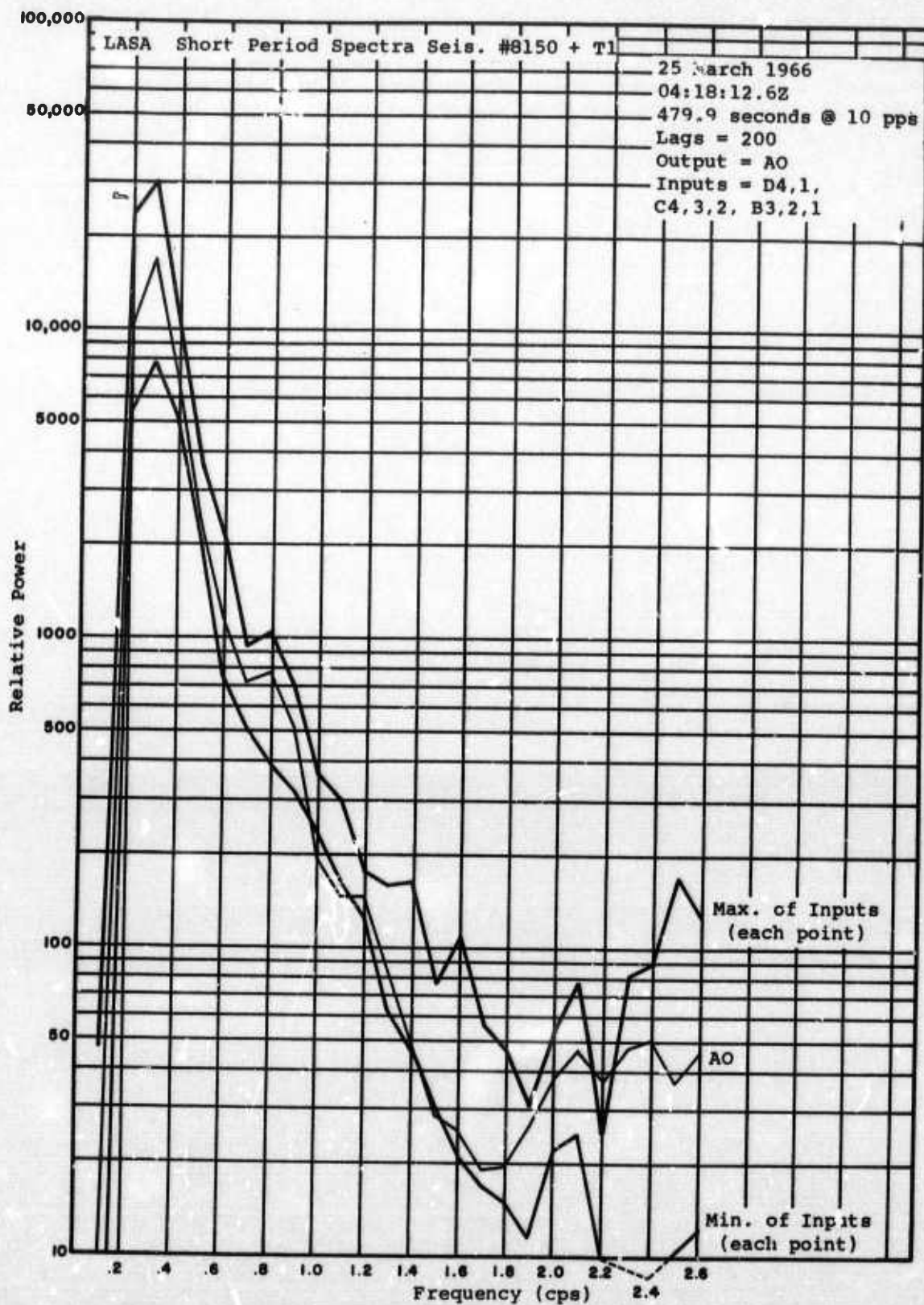


Figure 6. Output and range of input spectra for intersubarray samples used on Figure 1.

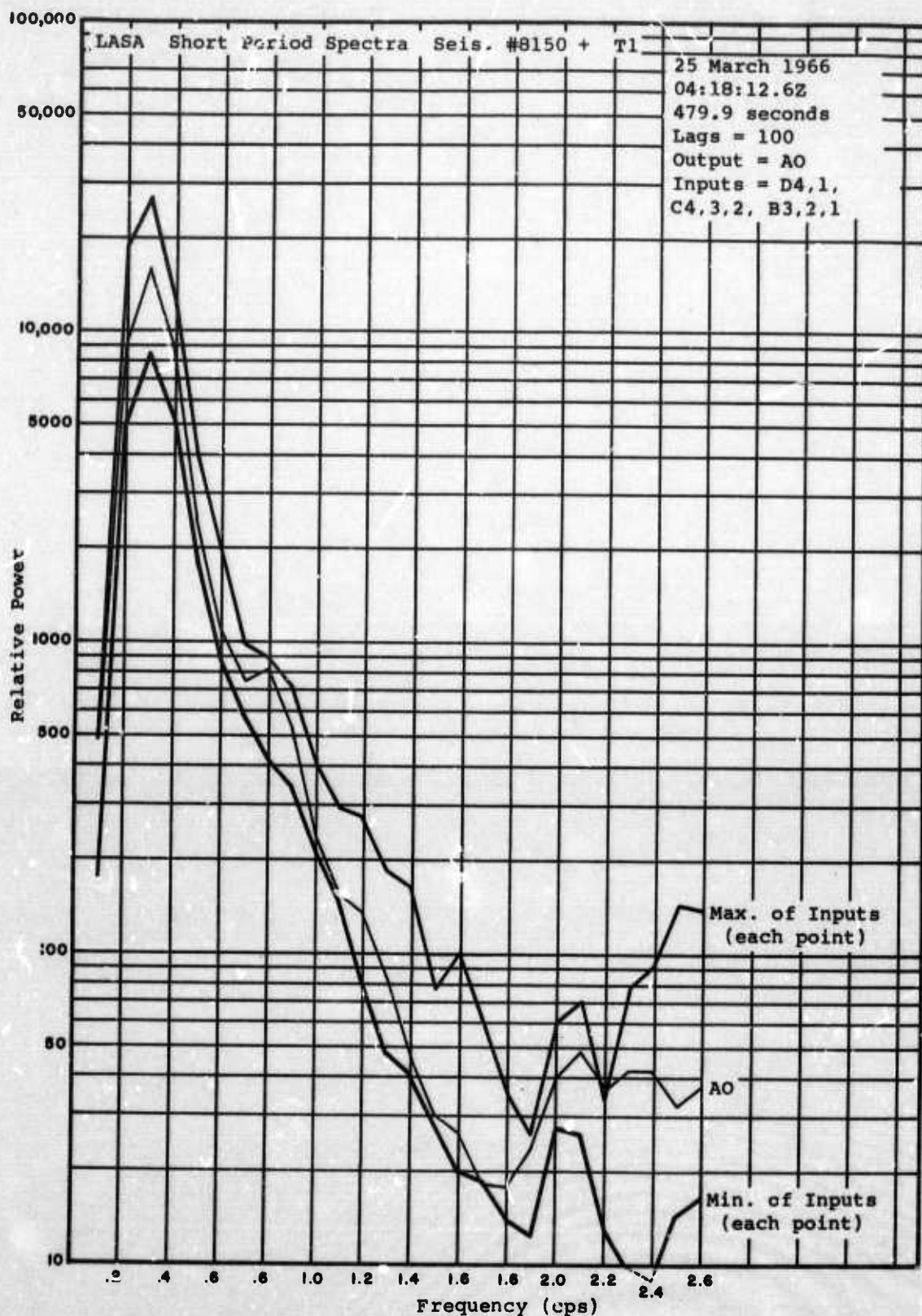


Figure 7. Output and range of input spectra for intersubarray samples used on Figure 1 but computed with 100 instead of 200 lags.

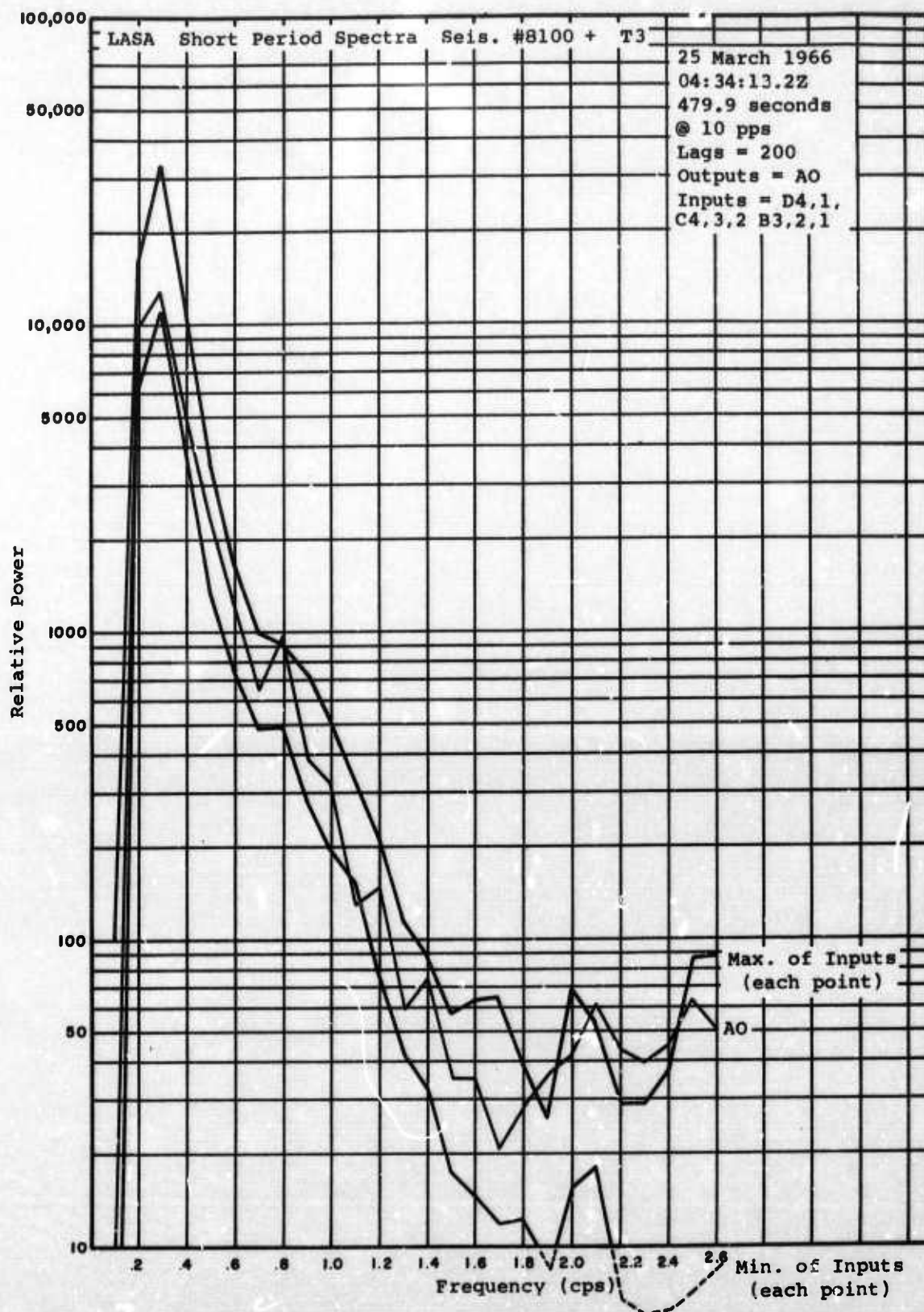


Figure 8. Output and range of input spectra for the third time sample similar to those presented on Figure 6.

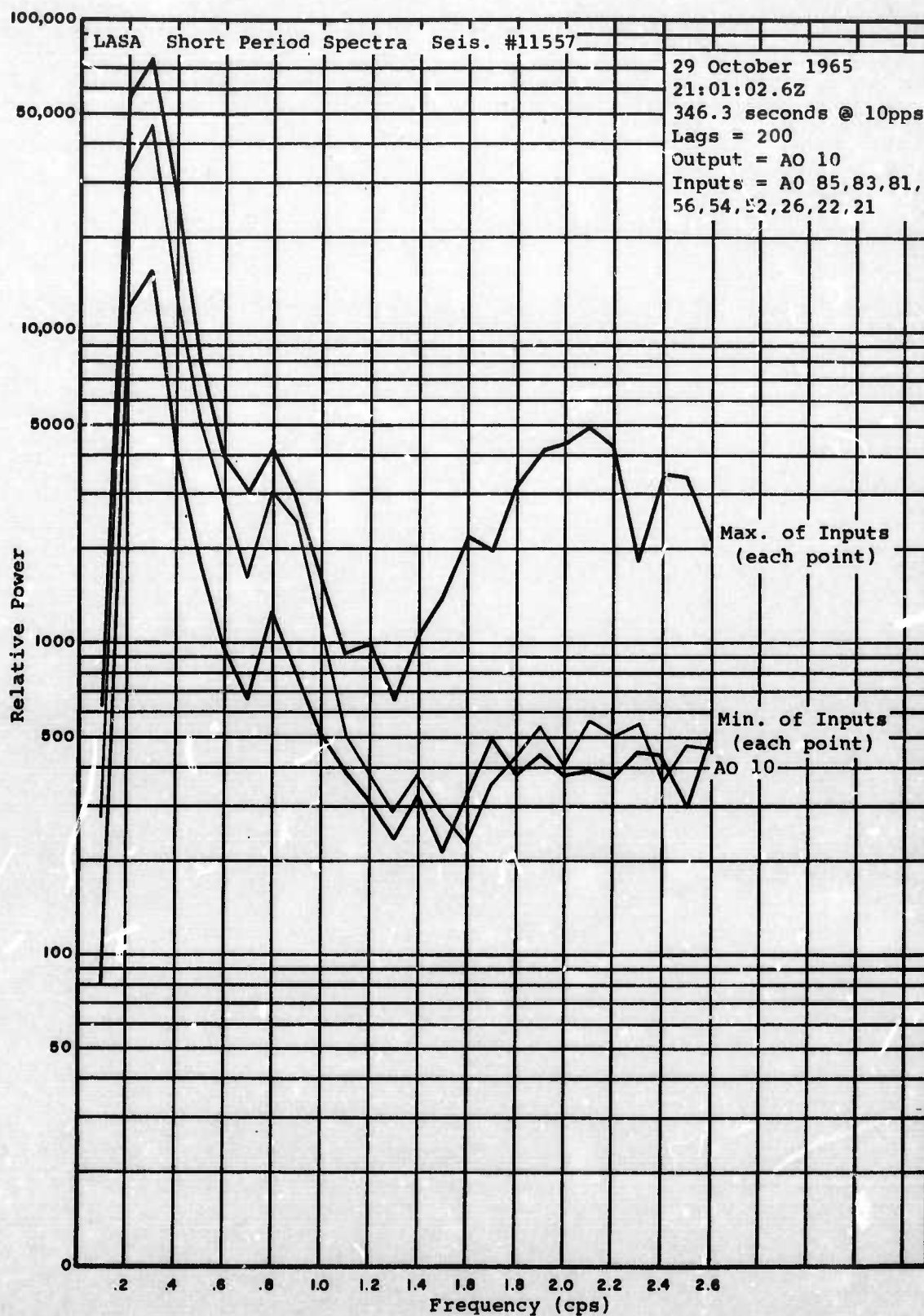


Figure 9. Output and range of input spectra for the intra-subarray noise immediately preceding the LONGSHOT event.

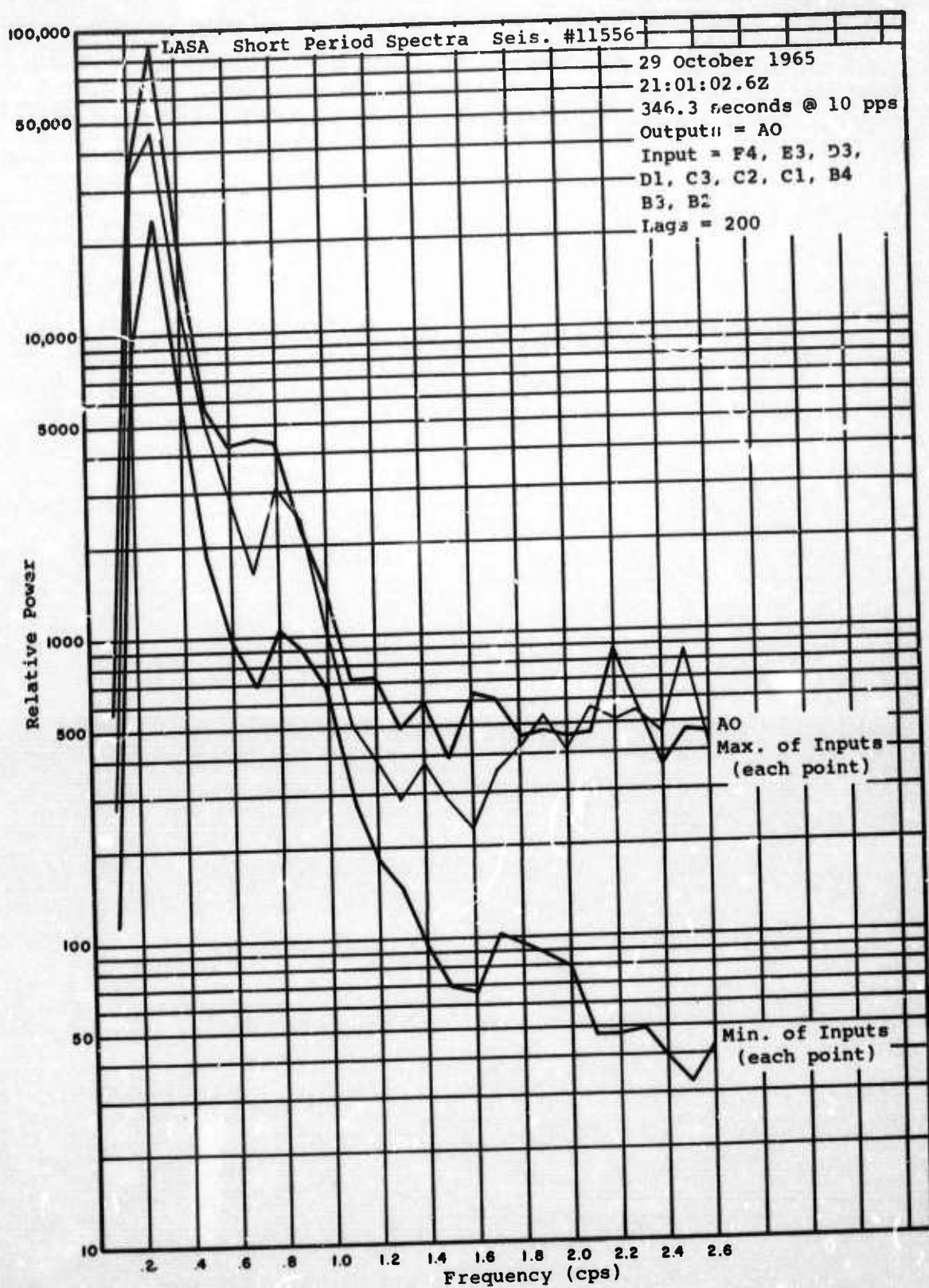


Figure 10. Output and range of input spectra for the inter-subarray noise immediately preceding the LONGSHOT event.

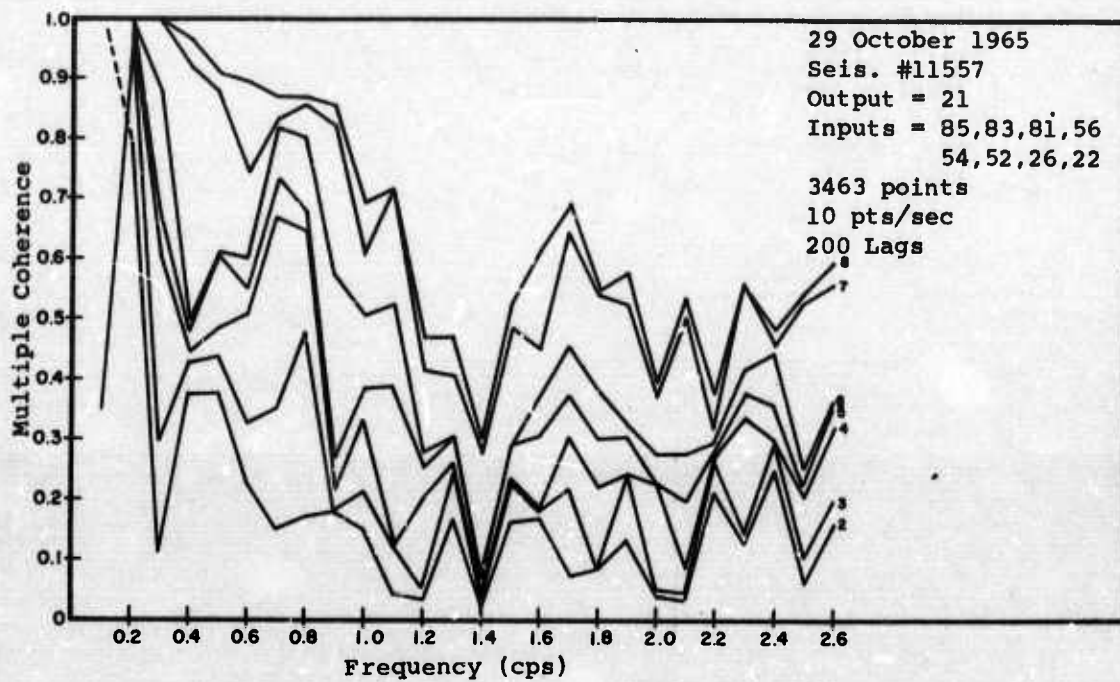


Figure 11. Intrasegment multiple coherence versus frequency when the output is from a seismometer in a 200 foot hole instead of the 500 foot hole at the subarray center.

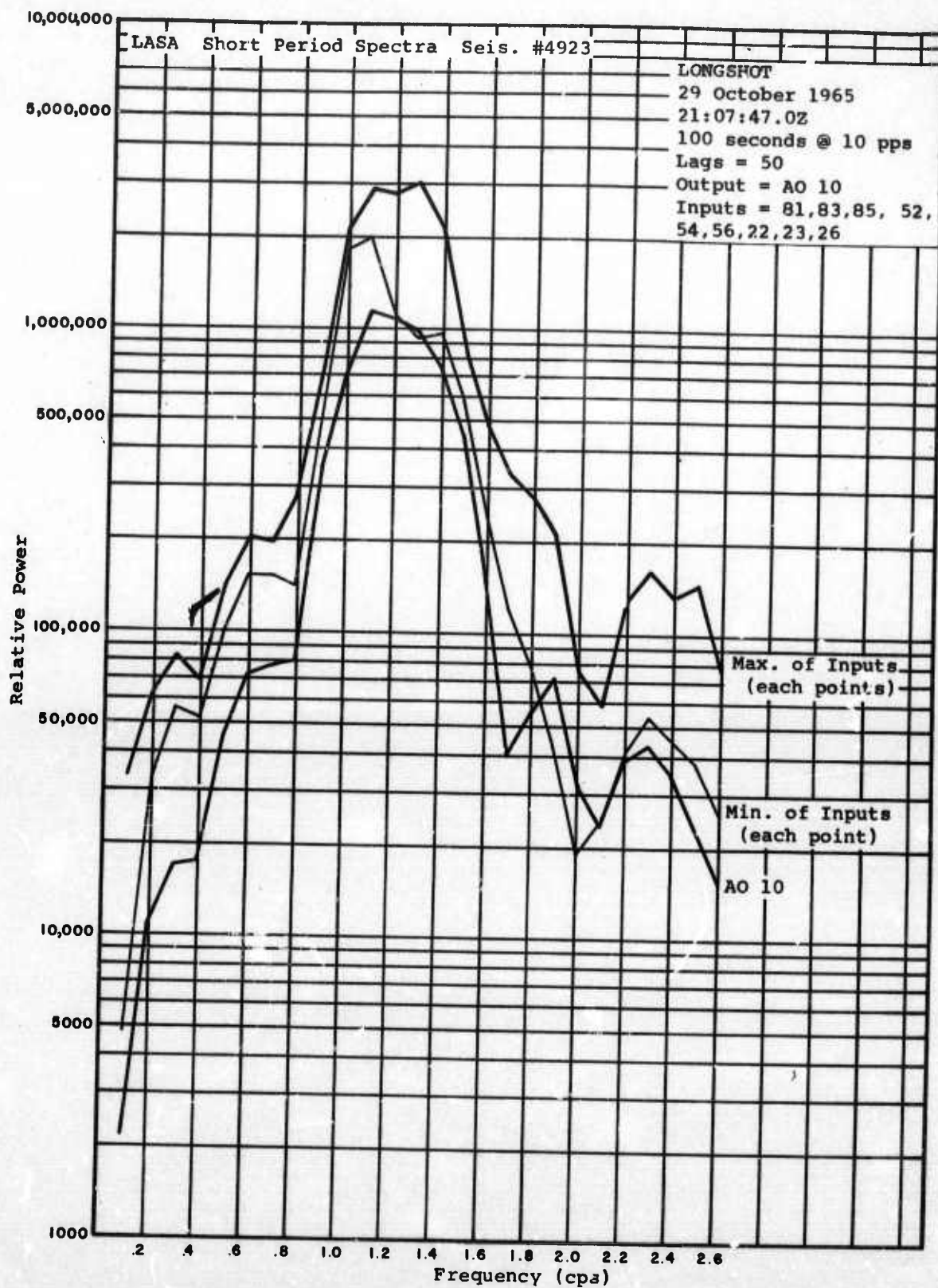


Figure 12. Output and range of input spectra for the interval including the LONGSHOT event.

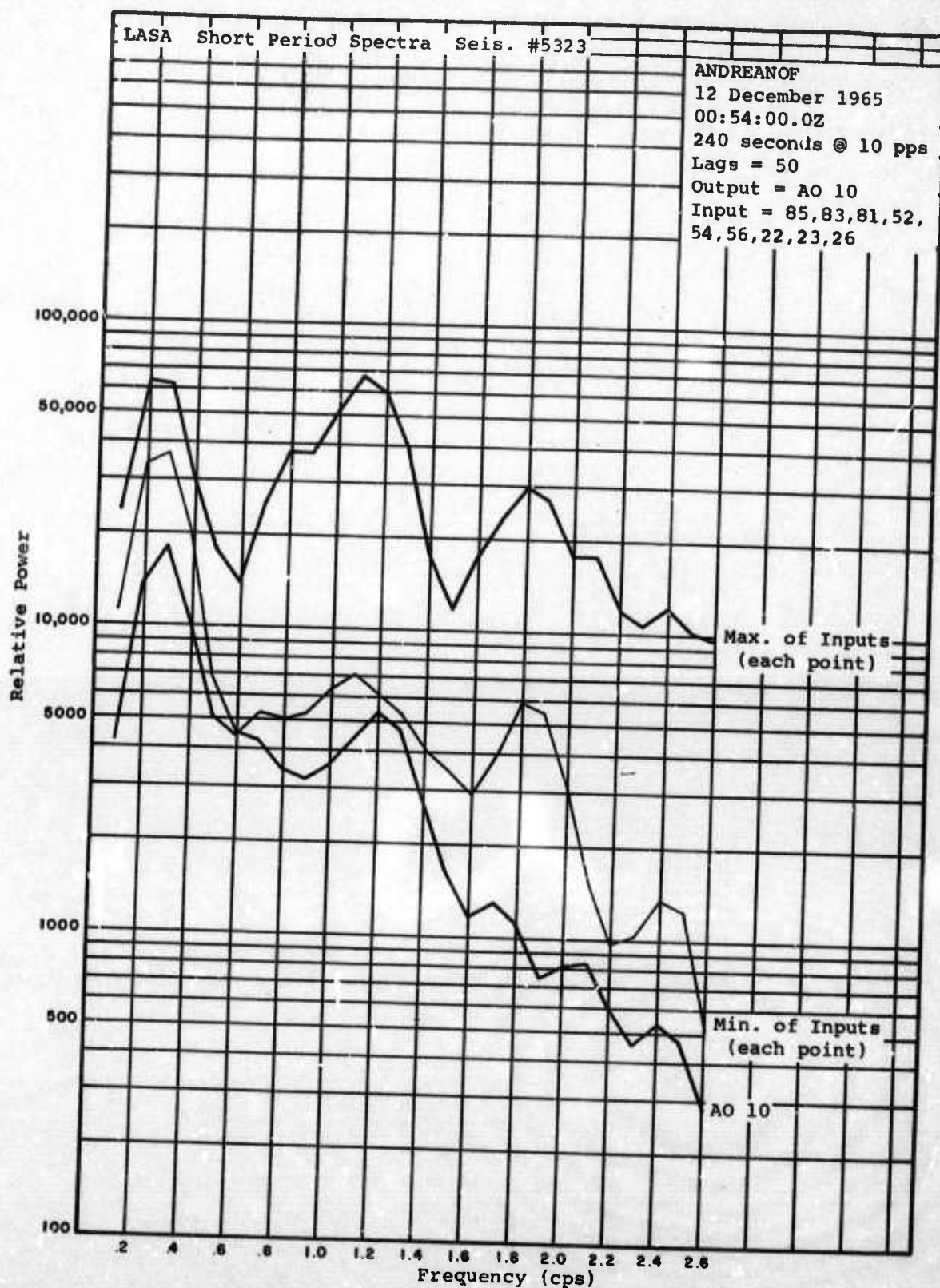


Figure 13. Output and range of input spectra for the interval including the Andreanof earthquake event.

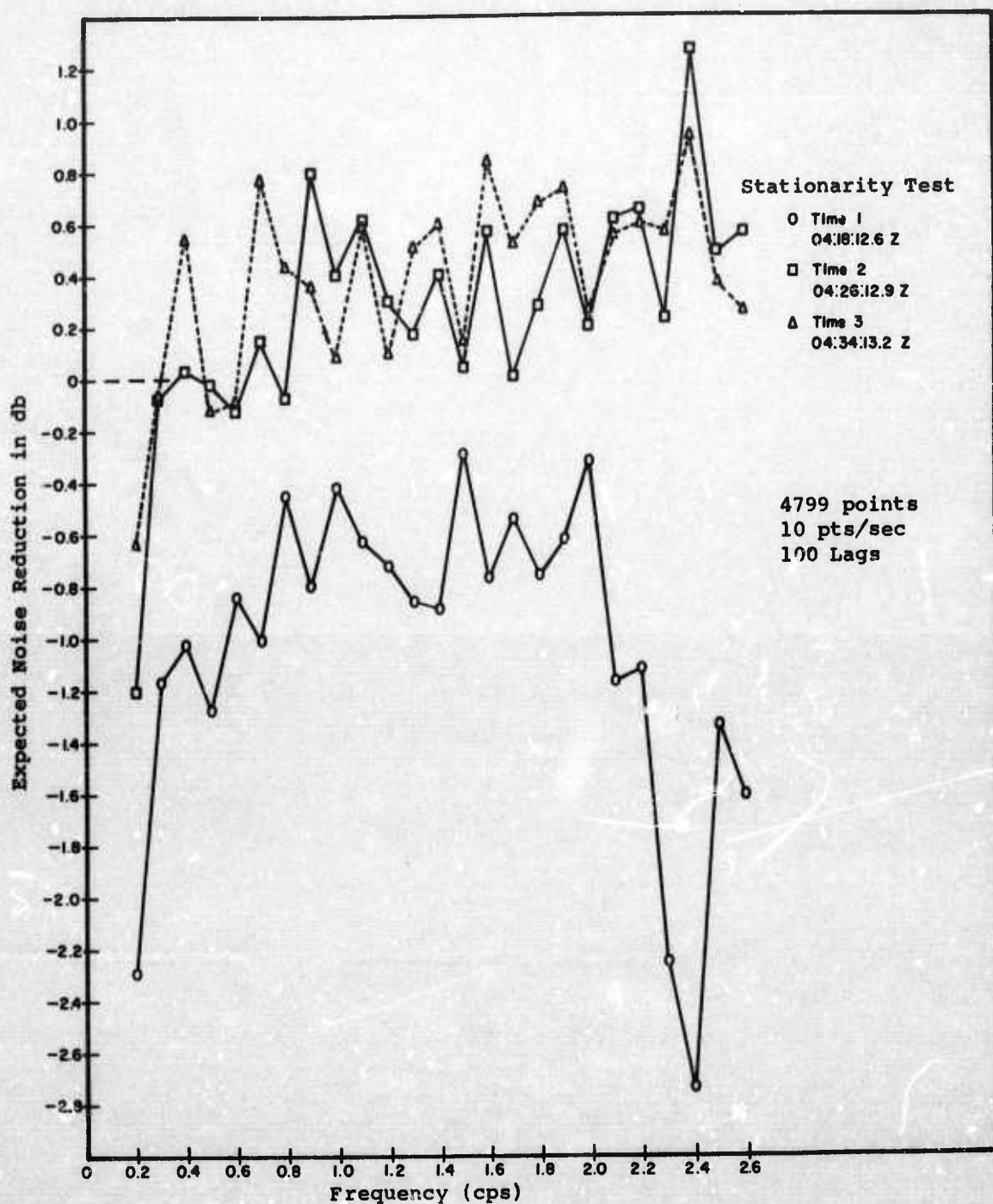


Figure 14. Expected noise reduction in db when a prediction error filter is applied to the fitting interval (Time 1) and the two adjacent intervals.

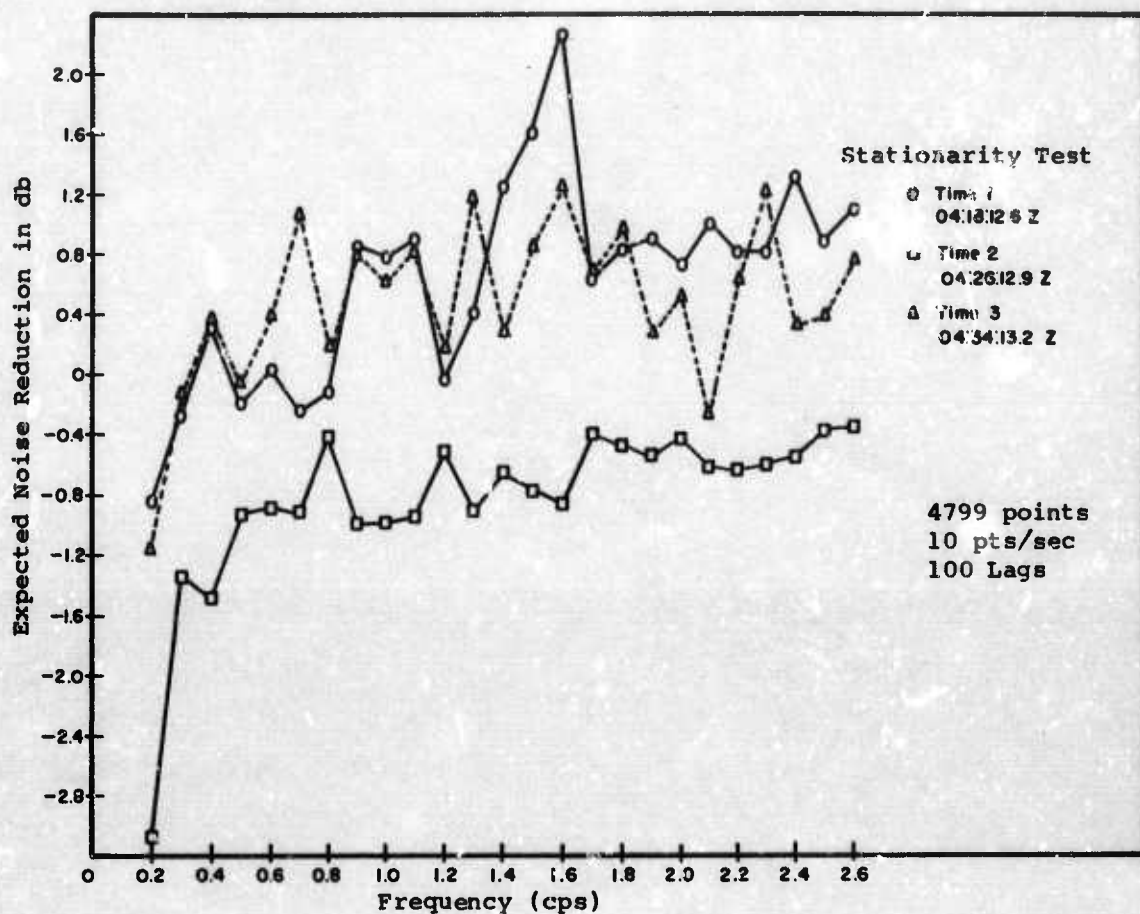


Figure 15. Expected noise reduction in db when a prediction error filter is applied to the fitting interval (Time 2) and the two adjacent intervals.

APPENDIX I

*Multiple Coherence Functions

Consider a collection of q clearly defined inputs $x_i(t)$; $i = 1, 2, \dots, q$, and one output $y(t)$, as pictured in Figure 5.12.

Let $G_i(f) = G_{ii}(f)$ be the

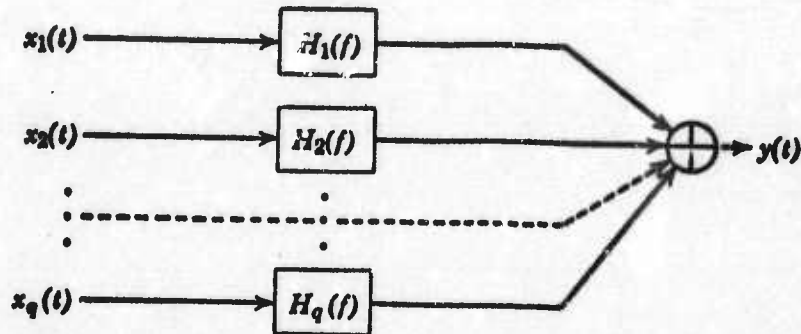


Figure 5.12 Multiple-input linear system.

power spectral density function for $x_i(t)$, and $G_{ij}(f)$ be the cross-spectral density function between $x_i(t)$ and $x_j(t)$. Define the $N \times N$ spectral matrix by

$$G_{xx}(f) = \begin{bmatrix} G_{11}(f) & G_{12}(f) & \cdots & G_{1q}(f) \\ G_{21}(f) & G_{22}(f) & & G_{2q}(f) \\ \vdots & \vdots & & \vdots \\ G_{q1}(f) & G_{q2}(f) & & G_{qq}(f) \end{bmatrix} \quad (1)$$

*This explanation of multiple coherence functions was taken from "Measurement and Analysis of Random Data", Bendat, J. S., and Piersol, A. G., John Wiley and Sons, 1966. For more detailed theoretical developments and discussions of multiple, partial and marginal coherence functions, see this text.

The ordinary coherence function between $x_i(f)$ and $x_j(t)$ is defined by

$$\gamma_{ij}^2(f) = \frac{|G_{ij}(f)|^2}{G_i(f) G_j(f)} \quad (2)$$

The multiple coherence function between $x_1(t)$ and all other inputs $x_1(t), x_2(t), \dots$, excluding $x_1(t)$, is defined by

$$\gamma_{1..}^2(f) = 1 - [G_{11}(f) G'(f)]^{-1} \quad (3)$$

where $G^i(g)$ denotes the i th diagonal element of the inverse matrix $G_{xx}(f)^{-1}$ associated with Eq. (1). The ordinary and multiple coherence functions are both real-valued quantities which are bounded by zero and unity. That is,

$$\begin{aligned} 0 &\leq \gamma_{ij}^2(f) \leq 1 \\ 0 &\leq \gamma_{1..}^2(f) \leq 1 \end{aligned} \quad (4)$$

The multiple coherence function is a measure of the linear relationship between the time history at one point, and the time histories at the collection of other points. That is, the multiple coherence function indicates whether or not the data at all of the other points linearly produce the results at a given point.

APPENDIX 2

Theoretical Development of The Stationarity Relations

A. Noise Reduction Within The Fitting Interval

A number of useful statistical measures such as ordinary and multiple coherence can be used as tools to indicate the amount of noise reduction feasible in a multiply coherent array. The basic linear model which determines the db reduction possible in the noise field by multiple coherence filtering relates a reference element (trace) $y(t)$ of an array to the other elements, say $x_1(t)$, $x_2(t)$, ..., $x_p(t)$ in the array through the linear model

$$y(t) = \sum_{k=1}^P \int_{-\infty}^{\infty} h_k(\alpha) x_k(t-\alpha) d\alpha \quad (1)$$

Generally we determine $h_k(t)$ as the time invariant linear filter that makes the mean square error between $y(t)$ and its predicted value a minimum, i. e.

$$E \left| y(t) - \sum_{k=1}^P \int_{-\infty}^{\infty} h_k(\alpha) x_k(t-\alpha) d\alpha \right|^2 = \min \quad (2)$$

which, by the usual orthogonality principle (see Papoulis 1), yields the condition

$$E y(t) x_l(t+\tau) = \sum_{k=1}^P \int_{-\infty}^{\infty} h_k(\alpha) E x_k(t-\alpha) x_l(t+\tau) d\alpha$$

$$l = 1, 2, \dots, p, -\infty < \tau < \infty \quad (3)$$

$$\text{or} \quad R_{yx_\ell}(\tau) = \sum_{k=1}^P \int h_k(\alpha) R_{x_k x_\ell}(\tau + \alpha) d\alpha \quad (4)$$

which by taking Fourier transforms implies that

$$S_{yx_\ell}(\omega) = \sum_{k=1}^P H_k^*(\omega) S_{x_k x_\ell}(\omega) \quad (5)$$

Now, the mean square error can be written

$$\begin{aligned} E|y(t) - \sum_{k=1}^P \int h_k(\alpha) x_k(t-\alpha) d\alpha|^2 &= E \left(y(t) - \sum_{k=1}^P \int_{-\infty}^{\infty} h_k(\alpha) x_k(t-\alpha) d\alpha \right) y(t) \\ &= R_{yy}(0) - \sum_{k=1}^P \int h_k(\alpha) R_{x_k y}(\alpha) d\alpha \\ &= \int_{-\infty}^{\infty} \left[S_{yy}(\omega) - \sum_{k=1}^P H_k^*(\omega) S_{x_k y}(\omega) \right] \frac{d\omega}{2\pi} \\ &= \int_{-\infty}^{\infty} \left(S_{yy} - S_{yx} S_{xx}^{-1} S_{xy} \right) (\omega) \frac{d\omega}{2\pi} \\ &= \int_{-\infty}^{\infty} \left(1 - \alpha^2(\omega) \right) S_{yy}(\omega) \frac{d\omega}{2\pi} \quad (6) \end{aligned}$$

where $\alpha^2(\omega)$ is the multiple coherence and $(1 - \alpha^2(\omega))$ measures the reduction in power possible at the frequency ω . With $\alpha^2(\omega) = 1$ the mean square error is zero and with $\alpha^2(\omega) = 0$ the mean square error is just

$$\int_{-\infty}^{\infty} S_{yy}(\omega) \frac{d\omega}{2\pi} = R_{yy}(0) = E|y(t)|^2 \quad (7)$$

which is the original power in the process $y(t)$. Now the quantity $(1 - \alpha^2(\omega)) S_{yy}(\omega)$ represents the residual power at each frequency after the best linear estimate of the form (1) has been subtracted out. Hence the db reduction in power at each frequency is just the ratio of the output power of the residual (see equation (2)) to the input power in $y(t)$ or

$$I_H(\omega) = 10 \log \frac{S_{ee}(\omega)}{S_{yy}(\omega)} = 10 \log (1 - \alpha^2(\omega)) \quad (8)$$

where $\alpha^2(\omega)$ is the multiple coherence and $S_{ee}(\omega)$ is the power spectrum of the error process

$$e(t) = y(t) - \sum_{k=1}^P \int_{-\infty}^{\infty} h_k(\alpha) x_k(t - \alpha) d\alpha \quad (9)$$

B. Noise Reduction Outside The Fitting Interval

We would also like to determine the noise reduction in db which would result from using a set of filters $g_k(t)$, $k=1, \dots, p$ which have been derived either from another fitting interval or from theoretical considerations. To accomplish this let $h_k(t)$ be the optimal filters for the time under investigation and let $g_k(t)$ be any other set of filters whose mean square error is to be compared with $h_k(t)$. The mean square error of the g filters can be written using the orthogonality principle as

$$E \left| y(t) - \sum_{k=1}^P \int_{-\infty}^{\infty} g_k(\alpha) x_k(t - \alpha) d\alpha \right|^2 =$$

$$\begin{aligned}
& E|y(t) - \sum_{k=1}^P \int_{-\infty}^{\infty} h_k(\alpha) x_k(t-\alpha) d\alpha + \sum_{k=1}^P \int_{-\infty}^{\infty} (h_k(\alpha) - g_k(\alpha)) x_k(t-\alpha) d\alpha|^2 \\
& = E|y(t) - \sum_{k=1}^P \int_{-\infty}^{\infty} h_k(\alpha) x_k(t-\alpha) d\alpha|^2 + E| \sum_{k=1}^P \int_{-\infty}^{\infty} (h_k(\alpha) - g_k(\alpha)) x_k(t-\alpha) d\alpha|^2 \\
& = \int_{-\infty}^{\infty} (1 - \alpha^2(\omega)) S_{YY}(\omega) \frac{d\omega}{2\pi} + \int_{-\infty}^{\infty} (\underline{H} - \underline{G})^* S_{XX}(\underline{H} - \underline{G})(\omega) \frac{d\omega}{2\pi} \\
& = \int_{-\infty}^{\infty} \left[(1 - \alpha^2(\omega)) + \frac{(\underline{H} - \underline{G})^* S_{XX}(\underline{H} - \underline{G})(\omega)}{S_{YY}(\omega)} \right] S_{YY}(\omega) \frac{d\omega}{2\pi} \quad (10)
\end{aligned}$$

Hence, if we call the new error $l'(t)$ we have

$$l'(t) = y(t) - \sum_{k=1}^P \int_{-\infty}^{\infty} g_k(\alpha) x_k(t-\alpha) d\alpha$$

with power spectrum $S_{l',l'}(\omega)$, the new value for the improvement in the $S_k(t)$ filters would be

$$I_G(\omega) = 10 \log \frac{S_{l',l'}(\omega)}{S_{YY}(\omega)} = 10 \log_S \left(1 - \alpha^2(\omega) + \frac{(\underline{H} - \underline{G})^* S_{XX}(\underline{H} - \underline{G})(\omega)}{S_{YY}(\omega)} \right) \quad (12)$$

Equation (12) shows that the improvement in the $g_k(t)$ filters is expressed in terms of the improvement in the $h_k(t)$ filters and a correction term which is zero when $\underline{H} = \underline{G}$.

The improvement values $I_H(w)$ and $I_G(w)$ in equations (8) and (12) are those shown in the main body of the report.

Reference

1. Papoulis, A., Probability, Random Variables, and Stochastic Processes, McGraw Hill, 1965.

Unclassified
Security Classification

DOCUMENT CONTROL DATA - R&D		
(Security classification of title, body of abstract and indexing annotation must be entered when the overall report is classified)		
1. ORIGINATING ACTIVITY (Corporate author)		2a. REPORT SECURITY CLASSIFICATION
TELEDYNE, INC. ALEXANDRIA, VIRGINIA		Unclassified
		2b. GROUP

3. REPORT TITLE		
MULTIPLE COHERENCE OF SHORT PERIOD NOISE AT LASA		
4. DESCRIPTIVE NOTES (Type of report and inclusive dates)		
Scientific		
5. AUTHOR(S) (Last name, first name, initial)		
E. F. Chiburis and W. C. Dean		
6. REPORT DATE	7a. TOTAL NO. OF PAGES	7b. NO. OF REFS
26 June 1967	37	1
8a. CONTRACT OR GRANT NO.	8b. ORIGINATOR'S REPORT NUMBER(S)	
F 33657-67-C-1313	190	
a. PROJECT NO.		
VELA T/6702		
c.	8b. OTHER REPORT NO(S) (Any other numbers that may be assigned this report)	
ARPA Order No. 624		
d. ARPA Program Code No. 5810		
10. AVAILABILITY/LIMITATION NOTICES		
This document is subject to special export controls and each transmittal to foreign governments or foreign national may be made only with prior approval of Chief, AFTAC.		
11. SUPPLEMENTARY NOTES		12. SPONSORING MILITARY ACTIVITY
-----		ADVANCED RESEARCH PROJECTS AGENCY NUCLEAR TEST DETECTION OFFICE WASHINGTON, D. C.
13. ABSTRACT		
<p>Multiple coherence gives a quantitative measure versus frequency of how well a linear combination of n input channels can match the (n + 1) st channel in a seismic array. If the inputs can match the output exactly then the multiple coherence is unity and only n channels are necessary to describe the noise field. This report shows multiple coherence versus frequency with 2 to 9 input channels for short period noise fields at LASA.</p> <p>Intersubarray noise from the center seismometers in the 500 foot holes at LASA shows low multiple coherence for all frequencies from 0.1 to 2.5 cps even with the closest subarrays represented. The intersubarray multiple coherence indicates that the expected noise reduction from a prediction error filter is about 1 db over the fitting interval and about 0 db outside the fitting interval.</p> <p>Intrasubarray noise has a high multiple coherence for frequencies of 1 cps and lower when some input channels are within $\frac{1}{2}$ km of the output channel. When the inputs are at least 2 km away, the multiple coherence is less than 0.8 for all but microseismic frequencies.</p>		

DD FORM 1473
1 JAN 64

Unclassified
Security Classification

Unclassified

Security Classification

14. KEY WORDS	LINK A		LINK B		LINK C	
	ROLE	WT	ROLE	WT	ROLE	WT
LASA Large Aperture Seismic Array						
Multiple Coherence						
Prediction Error						
Multi-channel filtering						
Noise Spectra						
Seismic Arrays						
Stationarity						

INSTRUCTIONS

1. **ORIGINATING ACTIVITY:** Enter the name and address of the contractor, subcontractor, grantee, Department of Defense activity or other organization (corporate author) issuing the report.

2a. **REPORT SECURITY CLASSIFICATION:** Enter the overall security classification of the report. Indicate whether "Restricted Data" is included. Marking is to be in accordance with appropriate security regulations.

2b. **GROUP:** Automatic downgrading is specified in DoD Directive 5200.10 and Armed Forces Industrial Manual. Enter the group number. Also, when applicable, show that optional markings have been used for Group 3 and Group 4 as authorized.

3. **REPORT TITLE:** Enter the complete report title in all capital letters. Titles in all cases should be unclassified. If a meaningful title cannot be selected without classification, show title classification in all capitals in parentheses immediately following the title.

4. **DESCRIPTIVE NOTES:** If appropriate, enter the type of report, e.g., interim, progress, summary, annual, or final. Give the inclusive dates when a specific reporting period is covered.

5. **AUTHOR(S):** Enter the name(s) of author(s) as shown on or in the report. Enter last name, first name, middle initial. If military, show rank and branch of service. The name of the principal author is an absolute minimum requirement.

6. **REPORT DATE:** Enter the date of the report as day, month, year, or month, year. If more than one date appears on the report, use date of publication.

7a. **TOTAL NUMBER OF PAGES:** The total page count should follow normal pagination procedures, i.e., enter the number of pages containing information.

7b. **NUMBER OF REFERENCES:** Enter the total number of references cited in the report.

8a. **CONTRACT OR GRANT NUMBER:** If appropriate, enter the applicable number of the contract or grant under which the report was written.

8b, 8c, & 8d. **PROJECT NUMBER:** Enter the appropriate military department identification, such as project number, subproject number, system numbers, task number, etc.

9a. **ORIGINATOR'S REPORT NUMBER(S):** Enter the official report number by which the document will be identified and controlled by the originating activity. This number must be unique to this report.

9b. **OTHER REPORT NUMBER(S):** If the report has been assigned any other report numbers (either by the originator or by the sponsor), also enter this number(s).

10. **AVAILABILITY/LIMITATION NOTICES:** Enter any limitations on further dissemination of the report, other than those

imposed by security classification, using standard statements such as:

- (1) "Qualified requesters may obtain copies of this report from DDC."
- (2) "Foreign announcement and dissemination of this report by DDC is not authorized."
- (3) "U. S. Government agencies may obtain copies of this report directly from DDC. Other qualified DDC users shall request through _____."
- (4) "U. S. military agencies may obtain copies of this report directly from DDC. Other qualified users shall request through _____."
- (5) "All distribution of this report is controlled. Qualified DDC users shall request through _____."

If the report has been furnished to the Office of Technical Services, Department of Commerce, for sale to the public, indicate this fact and enter the price, if known.

11. **SUPPLEMENTARY NOTES:** Use for additional explanatory notes.

12. **SPONSORING MILITARY ACTIVITY:** Enter the name of the departmental project office or laboratory sponsoring (paying for) the research and development. Include address.

13. **ABSTRACT:** Enter an abstract giving a brief and factual summary of the document indicative of the report, even though it may also appear elsewhere in the body of the technical report. If additional space is required, a continuation sheet shall be attached.

It is highly desirable that the abstract of classified reports be unclassified. Each paragraph of the abstract shall end with an indication of the military security classification of the information in the paragraph, represented as (TS), (S), (C), or (U).

There is no limitation on the length of the abstract. However, the suggested length is from 150 to 225 words.

14. **KEY WORDS:** Key words are technically meaningful terms or short phrases that characterize a report and may be used as index entries for cataloging the report. Key words must be selected so that no security classification is required. Identifiers, such as equipment model designation, trade name, military project code name, geographic location, may be used as key words but will be followed by an indication of technical content. The assignment of links, rules, and weights is optional.

Unclassified

Security Classification